Received: 22 January 2022 | Accepted: 23 February 2022

DOI: 10.1111/1759-7714.14381

ORIGINAL ARTICLE

WILEY

Identification of a novel circ_0001946/miR-1290/SOX6 ceRNA network in esophageal squamous cell cancer

Jianjun Wang | **Wenjian Yao** | **Jiwei Li** | **Quan Zhang** | **Li Wei**

Department of Thoracic Surgery, Henan Provincial People's Hospital, People's Hospital of Zhengzhou University, People's Hospital of Henan University, Zhengzhou, China

Correspondence
Li Wei, Department of Thoracic Surgery, Henan Provincial People's Hospital, People's Hospital of Zhengzhou University, People's Hospital of Henan University, No. 7, Weiwu Road, Jinshui District, Zhengzhou City, Henan, China.
Email: wlhnsrmyyxwk@163.com

Abstract

Background: Circular RNAs (circRNAs) can function as competing endogenous RNAs (ceRNAs) to impact the development of esophageal squamous cell cancer (ESCC). Human circ_0001946 has been identified as a potential anticancer factor in ESCC, yet our understanding of its molecular basis remains limited.

Methods: Circ_0001946, microRNA (miR)-1290 and SRY-box transcription factor 6 (SOX6) were quantified by quantitative reasl-time PCR (qRT-PCR) or immunoblotting. Cell proliferation was assessed by CCK-8 and EDU assays. Cell apoptosis and invasion were evaluated by flow cytometry and transwell assays, respectively. Cell migration was detected by transwell and wound-healing assays. The direct relationship between miR-1290 and circ_0001946 or SOX6 was determined by dual-luciferase reporter and RNA immunoprecipitation (RIP) assays. Xenograft model assays were used to assess the role of circ_0001946 in tumor growth.

Results: Circ_0001946 expression was attenuated in human ESCC, and circ_0001946 increase impeded cell proliferation, invasion, migration and enhanced apoptosis in vitro. Moreover, circ_0001946 increase diminished xenograft growth in vivo. Mechanistically, circ_0001946 bound to miR-1290, and re-expression of miR-1290 reversed circ_0001946-dependent cell properties. SOX6 was a miR-1290 target and it was responsible for the regulation of miR-1290 in cell properties. Furthermore, circ_0001946 functioned as a ceRNA to regulate SOX6 expression via miR-1290.

Conclusion: Our findings uncover an undescribed molecular mechanism, the circ_0001946/miR-1290/SOX6 ceRNA crosstalk, for the anti-ESCC activity of circ_0001946.

KEYWORDS
ceRNA, circ_0001946, ESCC, miR-1290, SRY-box transcription factor 6 (SOX6)

INTRODUCTION

Esophageal squamous cell cancer (ESCC) is a prevalent aggressive malignancy with an increasing incidence and a high mortality.[1,2] Although endoscopic resection, combined modality therapy and systemic therapy have controlled localized ESCC effectively, these therapies have limited utility in treating advanced ESCC.[2] Pivotal players of ESCC pathogenesis, including proteins and circular RNAs (circRNAs), are being intensively explored.[3–5] Knowing the functions of these players may contribute to developing targeted and personalized therapy in further medicine.

CircRNAs are a special type of single-stranded RNA biomolecules, in which the 5′ and 3′ ends are covalently linked resulting in a looped structure.[6] Work in a number of laboratories has unveiled that some circRNAs exhibit the function of microRNA (miRNA) sponges or competing endogenous RNAs (ceRNAs).[7,8] Recently, circRNAs have established roles via their ceRNA activity in impacting the establishment and progression of human tumors,[9] including ESCC.[4,5,10] Human circ_0001946 is originated in a process called back-splicing of exons of cerebellar degeneration related protein 1 (CDR1) and it has established a contradictory role in tumor biology.[11–13] Circ_0001946 is present at low levels in glioblastoma and lung

cancer and it operates as a potential anti-tumor factor in these cancers.[12,13] Conversely, circ_0001946 is overexpressed in colorectal cancer and exerts oncogenic activity in this disease via miR-135a-5p.[11] In ESCC, circ_0001946 has been discovered to be underexpressed and its dysregulation is associated with the recurrence and survival of ESCC.[14] Circ_0001946 expression increase suppresses ESCC cell malignant properties,[14] yet our understanding of its molecular circuitry that governs ESCC development remains limited.

Deregulated miRNA activity can contribute to esophageal tumorigenesis and ESCC progression.[15,16] Circulating miR-1290 has been proposed as a promising diagnostic marker of pancreatic cancer, colorectal cancer, and lung adenocarcinoma.[17–19] The strong carcinogenesis of miR-1290 has been reported in oral squamous cell carcinoma, glioma, and pancreatic ductal adenocarcinoma.[20–22] Moreover, miR-1290 is strongly upregulated in ESCC and it can work as an oncomir in this disease, suggesting miR-1290 may be a biomarker or therapeutic target in ESCC.[23–26]

SRY-box transcription factor 6 (SOX6), a HMG-box transcription factor, is underexpressed in the majority of human cancers, such as Ewing sarcoma, leukemia, and lung adenocarcinoma.[27–29] Functional studies in ESCC cell lines indicate that SOX6 has anticancer activity in ESCC.[30–33] Here, our findings support the suppressive activity of circ_0001946 in ESCC cell malignant phenotypes. Importantly, we uncover a new molecular circuitry, the circ_0001946/miR-1290/SOX6 ceRNA network, in the regulation of circ_0001946.

METHODS

Human specimens

We obtained 77 patient samples of primary ESCC at Henan Provincial People's Hospital, People's Hospital of Zhengzhou University, People's Hospital of Henan University between June 2018 and April 2021. The clinicopathological features of these patients are provided in Table 1. These patients had no treatment prior to surgery. All of the specimens had patient's informed consent and were histologically confirmed. Each tumor was paired with a normal esophageal tissue from the same patients. All specimens were used to analyze the expression of circ_0001946, miR-1290 and SOX6. Use of human specimens was approved by the Ethics Committee of Henan Provincial People's Hospital, People's Hospital of Zhengzhou University, People's Hospital of Henan University.

Cell lines

The ECA109 (Fenghuishengwu, Changsha, China) and KYSE450 (BeNa, Beijing, China) ESCC cell lines were grown in 10% FBS RPMI-1640 medium (Life Technologies). Human esophageal HET-1A cells (CRL-2692; ATCC) were grown in bronchial epithelial cell medium (BEGM BulletKit; Clonetics). Then, 293 T cells (CRL-3216, ATCC) were propagated under ATCC-formulated conditions.

For actinomycin D experiments, KYSE450 and ECA109 cells were grown in 10% FBS RPMI-1640 containing 5 μg/ml of actinomycin D (GlpBio) for 0–24 h. Cells were collected at 0, 4, 8, 12, and 24 h post-treatment for RNA expression analysis.

RNA isolation, RNase R treatment and expression analysis by quantitative real-time PCR (qRT-PCR)

For qRT-PCR, we extracted total RNA with the miRNeasy or RNEasy mini Kit from collected tissues and cultured cells as per the manufacturer's instructions (Qiagen). For RNase R experiments, 3 μg of total cellular RNA was either exposed to 0 units (control) or 10 units of RNase R (Lucigen) for 30 min at 37°C. After DNase treatment (TaKaRa), total RNA was processed to cDNA by reverse transcription (RT) using PrimeScript RT Kit from TaKaRa (for mRNAs and circ_0001946) or TaqMan RT Kit from Applied BioSystems (for miR-1290). Target sequences were amplified by SYBR-based qRT-PCR (Qiagen) and miRNA expression was assayed by the Applied BioSystem TaqMan miRNA Assay System. Sequences of qRT-PCR primer sets were included in Table S1. Expression of targets was determined by the $2^{-\Delta\Delta Ct}$ method relative to the reference gene β-actin (for mRNAs and circ_0001946) or U6 (for miR-1290).

Transient transfection and lentivirus transduction of cells

Human circ_0001946 sequence incorporated with EcoR I and BamH I sites (Sangon Biotech) was ligated into pLO5-ciR vector (Geneseed) after restriction digests to produce a recombinant plasmid expressing circ_0001946 (oe-circ_0001946). A scramble-plasmid served as a nonspecific control (vector). SOX6 expression was silenced by the SOX6-siRNA (si-SOX6, 5′-AUUCAUUGGUCGCUUAAU GUG-3′) and a siRNA-scramble served as the control siRNA (si-con). Chemically modified mimic of miR-1290, antisense nucleotide against miR-1290 (miR-1290 inhibitor) and two miRNA-scramble oligonucleotides (mimic NC and inhibitor NC) were supplied by Ribobio. For transient cell transfection, we plated KYSE450 and ECA109 cells (1×10^5 cells/well) into 12-well white TC dishes 24 h before transfection. We transfected the cells with 200 ng of plasmid and/or 50 nM of miRNA (mimic or inhibitor) and/or 100 nM of siRNA using lipofectamine RNAiMAX or 3000 as described by the manufacturer (Invitrogen). We harvested the transfected KYSE450 and ECA109 cells 24–96 h post-transfection for cell function and expression assays.

Circ_0001946-expressing lentivirus constructs (lenti-circ_0001946) and control lentivirus constructs were

TABLE 1 Correlations of circ_0001946, miR-1290, and SOX6 expression with the clinicopathological features of patients with esophageal squamous cell carcinoma (ESCC)

		circ_0001946			miR-1290			SOX6		
Characteristics	***n***	**High**	**Low**	***p***	**High**	**Low**	***p***	**High**	**Low**	***p***
Gender										
Male	40	21	19	0.565	18	22	0.427	16	24	0.088
Female	37	17	20		20	17		22	15	
Age										
<60	35	20	15	0.212	16	19	0.560	21	14	0.088
≥60	42	18	24		22	20		17	25	
Tumor size (cm)										
≦3	44	26	18	0.048*	17	27	0.030*	25	19	0.130
>3	33	12	21		21	12		13	20	
TNM stage										
I + II	45	27	18	0.027*	17	28	0.016*	28	17	0.007*
III + IV	32	11	21		21	11		10	22	
Differentiation										
Well and moderate	33	23	10	0.002*	22	11	0.008*	21	12	0.030*
Poor	44	15	29		16	28		17	27	
Lymph node metastasis										
Yes	38	26	12	0.001*	24	14	0.017*	25	13	0.004*
No	39	12	27		14	25		13	26	

Note: *$p < 0.05$, statistically significant.

supplied by Geneseed. We infected ECA109 cells with these lentivirus constructs at different vector doses ranging from 10^6 to 10^9 TU/ml. To obtain ECA109 cells stably expressing circ_0001946, cells were puromycin-selected for 10 days.

Cell proliferation analysis by cell counting kit-8 (CCK-8) and 5-ethynyl-2′-deoxyuridine (EDU) assays

Transfected KYSE450 and ECA109 cells (2×10^3 cells/well) were seeded into 96-well plastic dishes and grown under standard conditions for 0–72 h. In the CCK-8 assay, at 0, 24, 48 and 72 h post-seeding, we evaluated cell growth using CCK-8 solution following the manufacturer's recommendations (Yesen). Absorption at 450 nm was determined by spectrophotometry (TECAN). In the EDU assay, at 72 h after cell seeding, we treated the cells with Cell-Light EdU Apollo488 Kit (Ribobio) and 4′,6-diamidino-2-phenylindole (DAPI, Yesen) (nuclear staining) as previously described.[34] The proportion of EDU-positive cells was scored using a fluorescence microscope (Keyence).

Cell apoptosis analysis by flow cytometry

KYSE450 and ECA109 cells after 96 h various transfections were washed three times in cold PBS, stained with propidium iodide (PI, 50 μg/ml, MedChemExpress) and Annexin V-FITC (25 μg/ml, BD Biosciences) for 20 min in the dark, and analyzed within 1 h. A total of 1×10^4 events were scored using a BD LSRII cytometer and AccuriC6 software as recommended by the manufacturer (BD Biosciences).

Transwell invasion and migration assays

KYSE450 and ECA109 cells after 24 h various transfections were resuspended in 0.2% FBS media. The cells were plated on 8 micron 24-transwell inserts (Corning Costar) with (for invasion, 1×10^5 cells/well) or without (for migration, 3×10^4 cells/well) Matrigel (Corning Costar). Subsequently, the inserts were transferred into 24-well dishes with 600 μl of complete growth media and cell motility was allowed for 24 h. After being fixed by methanol and stained with 1% crystal violet, migratory or invasive cells were scored under a computerized Axiovert 200 M microscope (Zeiss).

Wound-healing assay for cell migration

We plated KYSE450 and ECA109 cells after 24 h various transfections in 6-well plastic dishes (5×10^5 cells/well). After cell seeding, an appropriate incubation period was allowed to yield ∼90% confluence. We subsequently made a scratch wound using sterile pipette tips (200 μl). Images were photographed under phase-contrast microscopy (Zeiss) and cell migration was expressed as the percentage of controls.

Immunoblotting

Individual tissue and cell lysates were prepared in RIPA with protease and phosphatase inhibitors (Thermo Fisher Scientific). Equivalent amounts of proteins were electrophoresed on 4%–20% gradient Tris–HCl gels (Bio-Rad) and resolved proteins were blotted to PVDF membranes (Roche). Antibodies (Invitrogen) for immunoblotting were as follows: rabbit SOX6 polyclonal (PA5-82125, 1:1000), mouse Bax monoclonal (33–6400, 1:1000), mouse Bcl-2 monoclonal (MA5-11757, 1:50), and mouse GAPDH monoclonal (39–8600, 1:500) antibodies. Bands were quantified by GelDoc software (Bio-Rad).

Bioinformatics and dual-luciferase reporter assay

We obtained the predicted miRNA-binding sites to circ_0001946 and human 3′untranslated regions (3′UTRs) from the web tool circInteractome[35] and TargetScan,[36] respectively. Human circ_0001946 fragment only encompassing a putative miR-1290 target sequence (Figure 3a) and SOX6 3′UTR were ligated into pMIR-REPORT vector (Ambion; Thermo Fisher Scientific) to produce wild-type reporter constructs (circ_0001946 wt and SOX6 3′UTR wt). The sequence of circ_0001946 segment and SOX6 3′UTR harboring the mutated miR-1290 seed region were subcloned into the reporter vector to acquire mutant-type reporter constructs (circ_0001946 mut and SOX6 3′UTR mut). We cotransfected 293 T cells in 12-well dishes using lipofectamine 3000 with 300 ng of individual firefly luciferase reporter, 50 nM of miRNA mimic, and 50 ng of pRL-TK Renilla luciferase vector (Promega). Then, 48 h later, cells were lysed and luciferase luminescence was gauged by the GloMax 20/20 luminometer as per the manufacturer's instructions (Promega).

RNA immunoprecipitation (RIP) assay

We incubated cell lysates prepared in RIPA with rabbit Argonaute2 (Ago2) monoclonal antibody (ab186733, 1:30; Abcam) or isotype IgG control (ab172730, 1:100, Abcam) for 3 h at 4°C before adding magnetic beads (A/G) (MedChemExpress) for an additional 3 h. We extracted Ago2-associated RNA from the beads to evaluate circ_0001946 and miR-1290 levels using qRT-PCR.

Xenograft model assay

Ten female BALB/C nude mice aged 6 weeks (Beijing Vital River Laboratory Animal Technology Co., Ltd., Beijing, China) were maintained in specific-pathogen-free conditions and used for xenograft studies following approval by the Animal Care and Use Committee of Henan Provincial People's Hospital, People's Hospital of Zhengzhou University, People's Hospital of Henan University. For xenograft formation, we gave each mouse a total volume of 200 μl PBS containing 5×10^6 lentivirus-transduced ECA109 cells by subcutaneous injection into the left flanks. Each group included five mice. Xenograft tumor growth rates were monitored weekly by evaluating volume under the use of the $0.5 \times (\text{length} \times \text{width}^2)$ formula. Four weeks later, we collected the xenograft tumors from the mice. Paraffin-embedded xenograft tumors were processed by immunohistochemistry using antibodies against ki-67 (ab15580, 1:100; Abcam), Bax (33–6400, 1:300; Invitrogen), Bcl-2 (MA5-11757, 1:50; Invitrogen), MMP9 (ab76003, 1:1000; Abcam), and MMP2 (ab86607, 1:100; Abcam), biotinylated anti-mouse or anti-rabbit IgG second antibody (ab64255 or ab64256, 1:100, Abcam) and 3,3-diaminobenzidine tetrahydrochloride solution (MedChemExpress), as described elsewhere.[37]

Statistical analysis

Unless otherwise noted, mean ± SEM values from 3 biological replicates (in triplicate) were presented in the graphs. We utilized a two-tailed Student's *t*-test or ANOVA with Tukey's multiple comparison test. We analyzed the expression correlation of variables in primary ESCC specimens using Pearson's correlation coefficients. A p-value of <0.05 was considered statistically significant (*).

RESULTS

Circ_0001946 expression suppresses proliferation, invasion, and migration and promotes apoptosis of ESCC cells in vitro

First, qRT-PCR was used to measure the expression of circ_0001946 in 77 ESCC tissue specimens and adjacent nontumor esophageal tissues from the same patients. Relative to its expression in normal esophageal tissues, circ_0001946 was reduced in human ESCC tissues (Figure 1a). The expression of circ_0001946 was then gauged in ESCC cells and nontumor HET-1A cells, and this analysis confirmed that circ_0001946 exhibited reduced expression in ECA109 and KYSE450 ESCC cells compared with the controls (Figure 1b). The unusual stability of circ_0001946 was evaluated by RNase R digestion and actinomycin D treatment. Circ_0001946, rather than the CDR1 linear mRNA, was resistant to RNase R (Figure 1c). Moreover, the level of the CDR1 linear mRNA appeared to be inhibited by actinomycin D, and circ_0001946 expression was refractory to inhibition by actinomycin D (Figure 1d). Additionally, circ_0001946 expression was significantly correlated with the tumor size, TNM stage, differentiation and lymph node metastasis of these tumors (Table 1).

Because of the downregulation of circ_0001946 in ESCC, we sought to determine whether ectopic circ_0001946 could affect ESCC cell biological behaviors. To do so, we generated circ_0001946-expressing cells by introducing a recombinant cDNA (oe-circ_0001946) into ECA109 and KYSE450 cells. Enforced expression of circ_0001946 upon oe-circ_0001946

transfection, validated by qRT-PCR (Figure 2a), impeded cell proliferation (Figure 2b,c) and enhanced cell apoptosis (Figure 2d) compared with the control group. Our immunoblotting results also supported cell apoptosis enhancement induced by circ_0001946 elevation, as presented by the augmentation of proapoptosis protein Bax and the reduction of antiapoptosis Bcl-2 protein in circ_0001946-expressing cells (Figure 2e). We next used transwell and wound-healing assays to examine the effect on cell migration and invasion. When stably expressed in ECA109 and KYSE450 cells, circ_0001946 elicited suppressed migration and invasion rates (Figure 2f–h). Collectively, these results indicate that circ_0001946 affects cell growth, invasion, motility and apoptosis in vitro.

Circ_0001946 directly binds to miR-1290

To identify the mechanism by which circ_0001946 affects cell growth, invasion, motility and apoptosis, we used the web tool circInteractome[35] to search the miRNAs that bind to circ_0001946. Among these candidates, we focused on miR-1290 because circ_0001946 was predicted to encompass 23 binding sites for miR-1290. We selected the binding site (Figure 3a) with the highest score (98) of context+ score percentile for further analysis. To validate the circ_0001946-miR-1290 relationship through the binding site, we adopted dual-luciferase reporter assays in 293 T cells, which do not express endogenous circ_0001946 (data not shown). The segment of circ_0001946 only harboring the predicted miR-1290 binding site was inserted into pMIR-REPORT vector. 293 T cells were cotransfected with a firefly luciferase reporter, pRL-TK Renilla luciferase vector and miR-1290 mimic. Cotransfection of miR-1290 mimic significantly repressed the luciferase activity of the wild-type reporter construct; however, mutation of the miR-1290 seed region abolished the repressive ability of miR-1290 (Figure 3b). MiRNAs post-transcriptionally regulate gene expression in the RNA-induced silencing complexes (RISCs) that also contain Ago2, a pivotal component of RISCs.[38] Hence, RIP experiments were done using an antibody against Ago2. Consistent with miR-1290 localization, circ_0001946 could be present in the RISCs of ECA109 and KYSE450 cells (Figure 3c). Analysis of miR-1290 expression in ESCC tissue specimens revealed that miR-1290 was enhanced in ESCC tissues compared with the nontumor controls (Figure 3d). Intriguingly, there existed a clear inverse correlation between circ_0001946 and miR-1290 levels in ESCC tissue specimens (Figure 3e). Moreover, ECA109 and KYSE450 ESCC cells exhibited higher levels of miR-1290 compared with the nontumor HET-1A cells (Figure 3f). Furthermore, the expression of miR-1290 was closely associated with the tumor size, TNM stage, differentiation and lymph node metastasis of these tumors (Table 1). Together, these data suggest that circ_0001946 can bind to miR-1290.

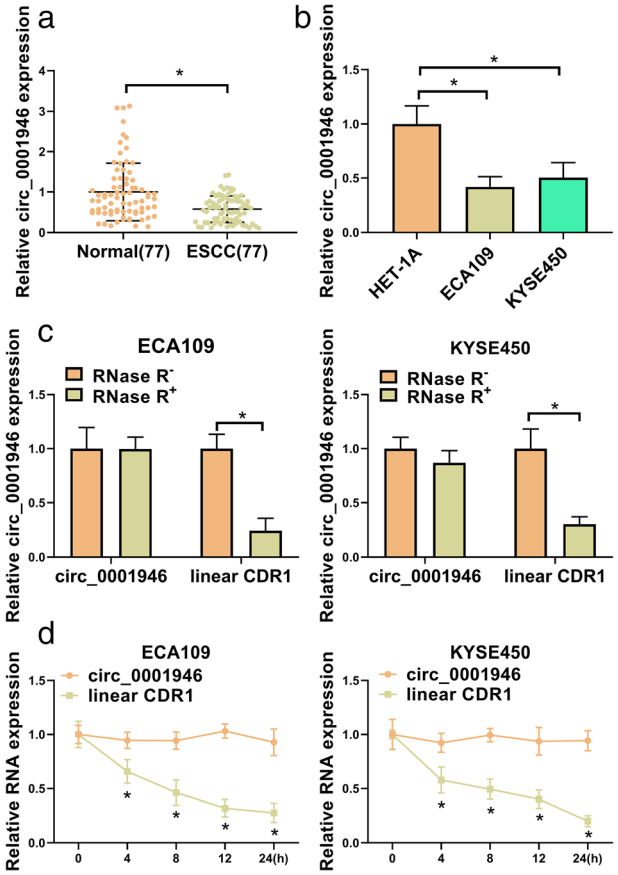

FIGURE 1 Circ_0001946 expression is attenuated in human ESCC. (a) qRT-PCR showing the downregulation of circ_0001946 in 77 ESCC tissue specimens compared with the adjacent nontumor esophageal tissues from the same patients. (b) qRT-PCR showing the reduction of circ_0001946 expression in ECA109 and KYSE450 ESCC cells compared with the nontumor HET-1A cells. (c) Effect of RNase R digestion on the levels of circ_0001946 and CDR1 linear mRNA. (d) Effect of actinomycin D treatment on the expression of circ_0001946 and CDR1 linear mRNA in ECA109 and KYSE450 ESCC cells. *$p < 0.05$

Re-expression of miR-1290 reverses circ_0001946-dependent cell proliferation, invasion, migration and apoptosis in vitro

The miR-1290 increase efficacy of miRNA mimic introduction was confirmed by qRT-PCR (Figure 4a). Intriguingly, in circ_0001946-expressing ECA109 and KYSE450 cells, we observed a clear downregulation in the expression of miR-1290 (Figure 4b). To determine whether in vitro phenotypes associated with circ_0001946 could be reversed via restoration of miR-1290, we transfected circ_0001946-expressing cells with miR-1290 mimic. Transfection of miR-1290 mimic strikingly restored the expression of miR-1290 reduced by circ_0001946 (Figure 4b). In circ_0001946-expressing ECA109 and KYSE450 cells, restoration of miR-1290 reversed, at least partially, circ_0001946-imposed proliferation defect (Figure 4c,d) and apoptosis promotion (Figure 4e,f). Furthermore, restoration of miR-1290 significantly rescued circ_0001946-driven migration and invasion defects (Figure 4g–i). In summary, these findings suggest that the ability of circ_0001946 to affect ESCC cell properties is attributable, in part, to its capacity to downregulate miR-1290.

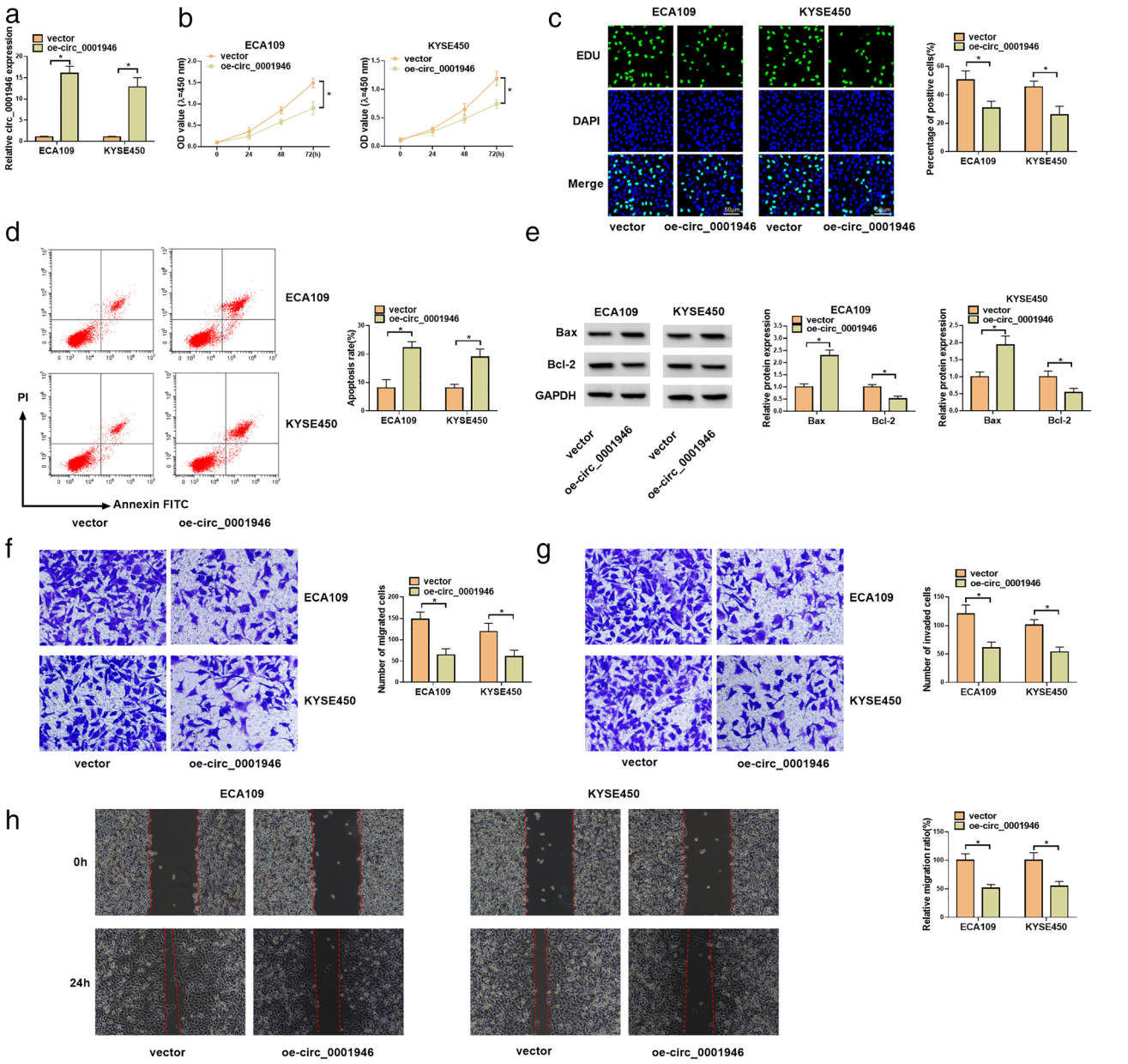

FIGURE 2 Circ_0001946 expression affects cell proliferation, invasion, migration and apoptosis in vitro. (a–h) ECA109 and KYSE450 cells were introduced with vector control or a recombinant plasmid expressing circ_0001946 (oe-circ_0001946). (a) qRT-PCR validating the circ_0001946 upregulation efficacy of oe-circ_0001946 transfection in ECA109 and KYSE450 cells. (b) CCK-8 assay with transfected ECA109 and KYSE450 cells to assess cell proliferation. (c) Representative EDU assay showing cell proliferation ability performed in transfected ECA109 and KYSE450 cells. (d) Representative images showing a cell apoptosis assay and flow cytometry with transfected ECA109 and KYSE450 cells. (e) Representative immunoblotting analysis showing the levels of Bax and Bcl-2 in transfected ECA109 and KYSE450 cells. (f and g) Representative transwell assay presenting cell migration and invasion rates performed in transfected ECA109 and KYSE450 cells. (h) Representative pictures depicting a cell migration assay performed by wound-healing assay with transfected ECA109 and KYSE450 cells. *$p < 0.05$

MiR-1290 directly targets SOX6 and circ_0001946 involves the regulation of SOX6 expression via miR-1290

To further understand the role of miR-1290, we identified its downstream effectors using the computer algorithm TargetScan[36] based on the presence of miR-1290 binding sites in their 3′UTRs. Among these potential targets, we focused on SOX6 because it has been shown to exert a tumor-suppressive function in human ESCC by impacting cancer cell apoptosis and proliferation.[30,31,39] The 3′UTR of SOX6 mRNA was predicted to have a putative miR-1290 pairing site (Figure 5a). The ability of miR-1290 to regulate SOX6 3′UTR was examined by dual-luciferase reporter assays. Reporter assays with miR-1290-expressing 293 T cells showed that miR-

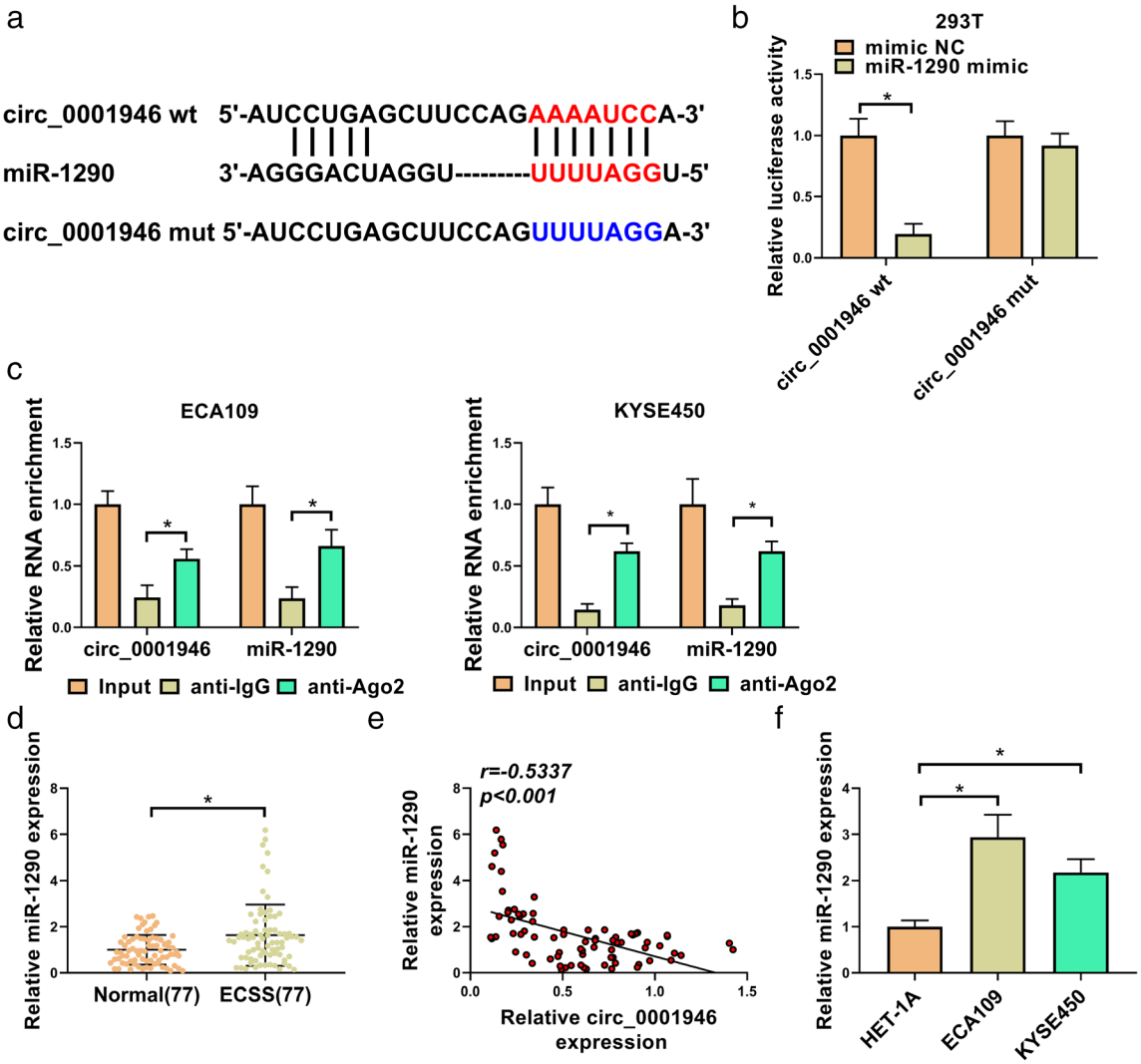

FIGURE 3 Circ_0001946 binds to miR-1290. (a) Schematic representation of the miR-1290 target sequence within circ_0001946. The predicted miR-1290 seed region was mutated. (b) The firefly luciferase reporter constructs with the wild-type (circ_0001946 wt) or mutant-type (circ_0001946 mut) miR-1290 seed region were cotransfected in 293 T cells along with pRL-TK Renilla luciferase vector and miR-1290 mimic or mimic mock. Cotransfection of miR-1290 mimic repressed the luciferase activity of circ_0001946 wt not circ_0001946 mut. (c) Lysates were incubated with anti-IgG or anti-Ago2 antibody and magnetic beads. qRT-PCR showing the enrichment levels of circ_0001946 and miR-1290 in Ago2-associated RNA. (d) qRT-PCR showing the overexpression of miR-1290 in 77 ESCC tissue specimens compared with the adjacent nontumor esophageal tissues from the same patients. (e) Scatter plots of miR-1290 expression versus circ_0001946 level in 77 ESCC tissue specimens. Pearson's correlation coefficients (r) and *p*-values are shown. (f) qRT-PCR showing the elevation of circ_0001946 expression in ECA109 and KYSE450 ESCC cells compared to the nontumor HET-1A cells. $^*p < 0.05$

1290 suppressed SOX6 3′UTR; mutation of the putative miR-1290 seed region abolished responsiveness to miR-1290 (Figure 5b), indicating the targeting of SOX6 by miR-1290. Moreover, in ESCC tissues, SOX6 mRNA was markedly repressed compared to the controls (Figure 5c). The strong inverse correlation between SOX6 mRNA and miR-1290 expression in ESCC tissues also supported the targeting of SOX6 by miR-1290 (Figure 5d). In line with mRNA expression, SOX6 protein level was strongly decreased in ESCC tissues and cells (Figure 5e,f). Moreover, the expression of SOX6 mRNA was closely associated with the tumor size, TNM stage, differentiation and lymph node metastasis of these tumors (Table 1).

The preceding observations established that circ_0001946 and SOX6 3′UTR bind to miR-1290 via a shared binding sequence (UUUUAGG) within miR-1290. We next asked if circ_0001946 involves the post-transcriptional SOX6 mRNA regulation via miR-1290. To do this, we transfected circ_0001946-expressing cells with or without miR-1290 mimic and examined SOX6 protein level by immunoblotting. Overexpression of circ_0001946 by oe-circ_0001946 transfection led to enhanced protein level of SOX6 in ECA109 and KYSE450 cells; restoration of miR-1290 significantly abrogated circ_0001946-mediated augmentation of SOX6 protein (Figure 5g). Hence, circ_0001946 can post-transcriptionally regulate SOX6 expression via miR-1290 competition.

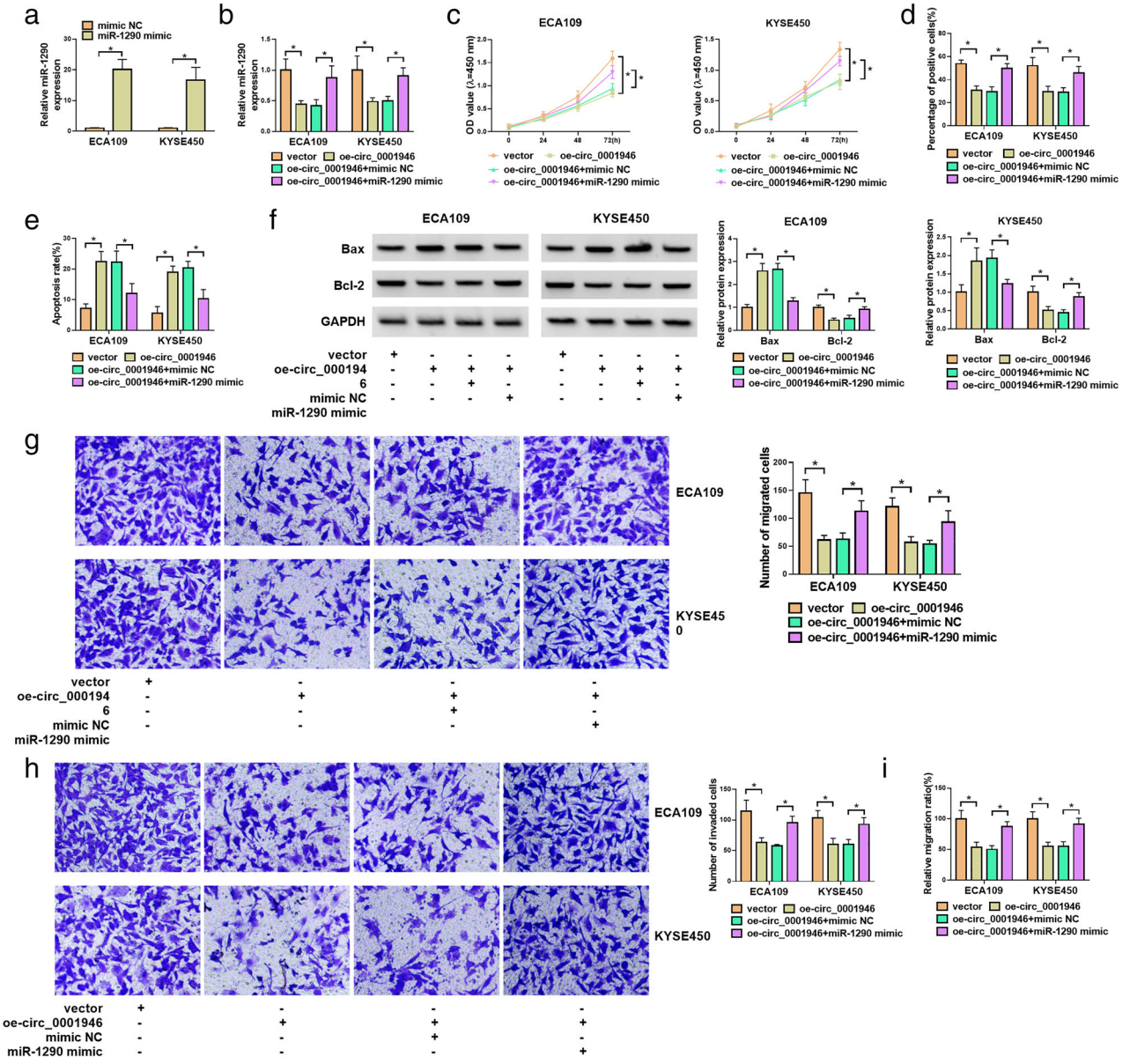

FIGURE 4 Reduction of miR-1290 underlies circ_0001946-dependent phenotypes in vitro. (a) qRT-PCR revealing the miR-1290 increase efficacy of miRNA mimic introduction in ECA109 and KYSE450 cells. (b) qRT-PCR for miR-1290 expression in circ_0001946-expressing or control ECA109 and KYSE450 cells transfected with or without miR-1290 mimic or mimic NC. (c) Proliferation analysis by CCK-8 assay with circ_0001946-expressing or control ECA109 and KYSE450 cells transfected as indicated. (d) Proliferation analysis by EDU assay with circ_0001946-expressing or control ECA109 and KYSE450 cells transfected as indicated. (e) Apoptosis assessment by flow cytometry with circ_0001946-expressing or control ECA109 and KYSE450 cells transfected as indicated. (f) Representative immunoblotting analysis showing Bax and Bcl-2 levels in circ_0001946-expressing or control ECA109 and KYSE450 cells transfected as indicated. (g and h) Representative migration (g) and invasion (h) analyses by transwell assay with circ_0001946-expressing or control ECA109 and KYSE450 cells transfected as indicated. (i) Migration evaluation by wound-healing assay with circ_0001946-expressing or control ECA109 and KYSE450 cells transfected as indicated. *$p < 0.05$

SOX6 is a downstream effector of miR-1290 in affecting cell proliferation, invasion, migration and apoptosis in vitro

To ascertain whether SOX6 represents a functional target of miR-1290, we downregulated miR-1290 with miRNA inhibitor in ECA109 and KYSE450 cells along with or without a siRNA specific to SOX6 (si-SOX6). The miR-1290 downregulation efficacy of miRNA inhibitor was validated by qRT-PCR (Figure 6a), and the transfection efficiency of si-SOX6 in suppressing SOX6 was verified by immunoblotting (Figure 6b). In miR-1290-silenced ECA109 and KYSE450 cells, SOX6 protein expression was enhanced (Figure 6c), supporting the notion that miR-1290 targets SOX6. Moreover, cotransfection of si-SOX6 reduced SOX6 protein expression induced by miR-1290

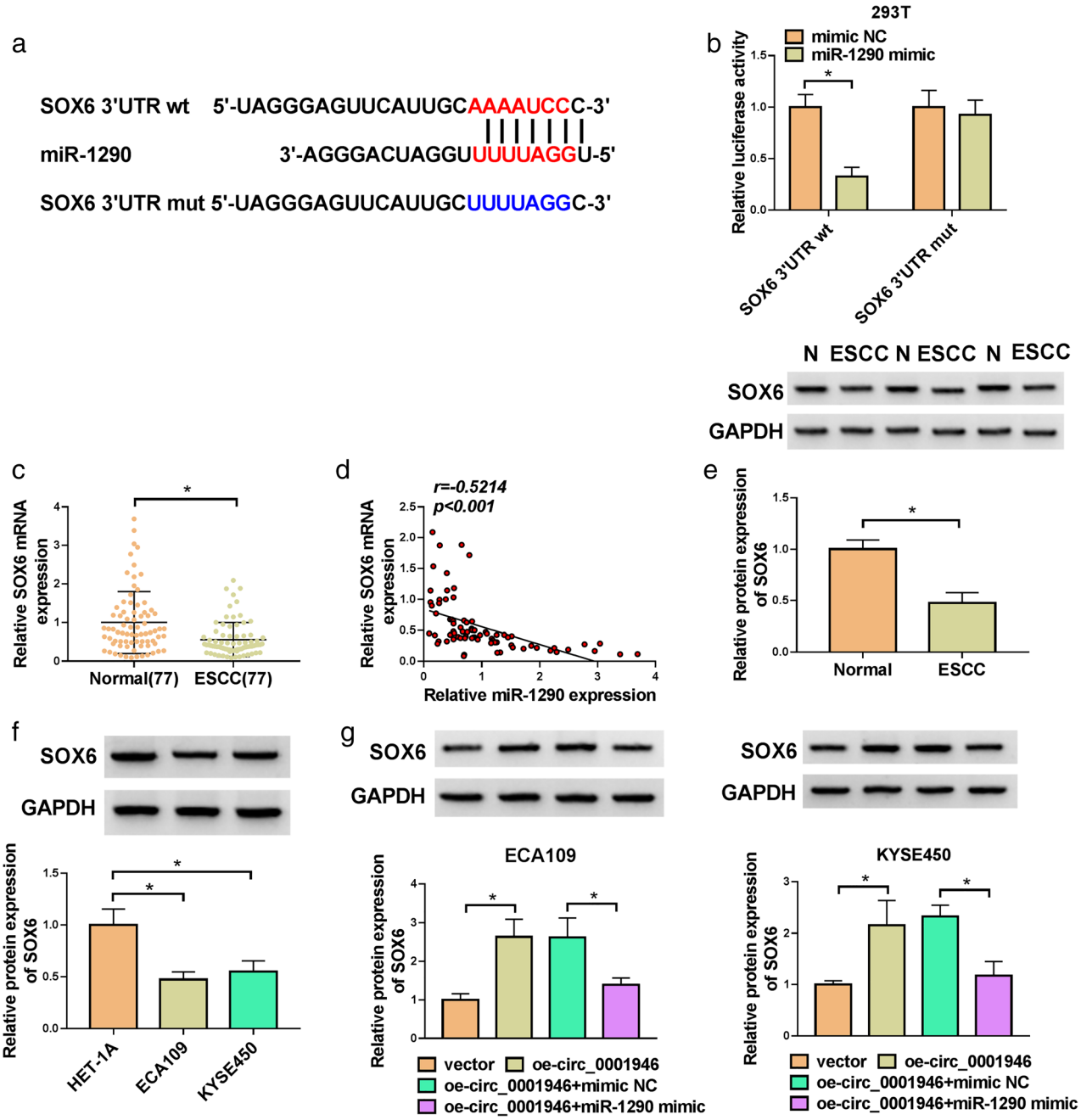

FIGURE 5 Circ_0001946 regulates SOX6 expression via miR-1290 competition. (a) Schematic representation of the miR-1290 target sequence within SOX6 3′UTR. The predicted miR-1290 seed sequence was mutated. (b) Firefly luciferase reporter constructs with the wild-type (SOX6 3′UTR wt) or mutant-type (SOX6 3′UTR mut) miR-1290 target sequence were cotransfected in 293 T cells along with pRL-TK Renilla luciferase vector and miR-1290 mimic or mimic mock. Cotransfection of miR-1290 mimic repressed the luciferase activity of SOX6 3′UTR wt not SOX6 3′UTR mut. (c) qRT-PCR showing the reduction of SOX6 mRNA in 77 ESCC tissue specimens compared with the adjacent nontumor esophageal tissues from the same patients. (d) Scatter plots of SOX6 mRNA level versus miR-1290 expression in 77 ESCC tissue specimens. Pearson's correlation coefficients (r) and *p*-values are shown. (e) Representative immunoblotting analysis showing the downregulation of SOX6 protein level in three ESCC tissue specimens compared to the three normal esophageal tissues from the same patients. (f) Representative immunoblotting analysis presenting the reduction of SOX6 protein level in ECA109 and KYSE450 ESCC cells compared to the nontumor HET-1A cells. (g) Representative immunoblotting analysis revealing SOX6 protein level in circ_0001946-expressing or control ECA109 and KYSE450 cells transfected with or without miR-1290 mimic or mimic NC. *$p < 0.05$

depletion (Figure 6c). Remarkably, miR-1290 depletion suppressed cell proliferation (Figure 6d,e) and accelerated cell apoptosis (Figure 6f,g), as well as impeded cell migration and invasion (Figure 6h–j) in ECA109 and KYSE450 cells; reduction of SOX6 protein partly abolished these effects of miR-1290 depletion (Figure 6d–j). All these results indicate that SOX6 seems to be a downstream effector of miR-1290.

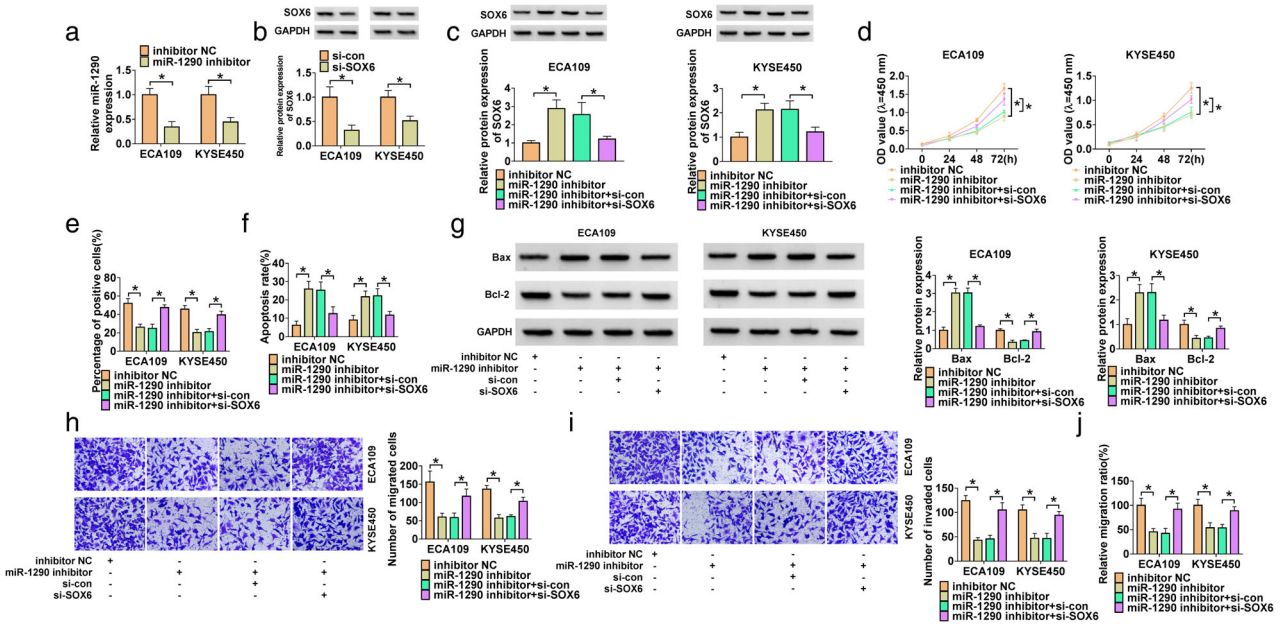

FIGURE 6 SOX6 is a downstream effector of miR-1290. (a) qRT-PCR showing the miR-1290 downregulation efficacy of miR-1290 inhibitor transfection. (b) Representative immunoblotting analysis revealing the transfection efficiency of si-SOX6 in suppressing SOX6. (c–j) ECA109 and KYSE450 cells were transiently introduced with si-SOX6 + miR-1290 inhibitor, si-con+miR-1290 inhibitor, miR-1290 inhibitor or inhibitor NC. (c) Representative immunoblotting analysis showing SOX6 protein level in transfected ECA109 and KYSE450 cells. (d) Proliferation analysis by CCK-8 assay with transfected ECA109 and KYSE450 cells. (e) Proliferation analysis by EDU assay with transfected ECA109 and KYSE450 cells. (f) Apoptosis assessment by flow cytometry with transfected ECA109 and KYSE450 cells. (g) Representative immunoblotting analysis showing Bax and Bcl-2 levels in transfected ECA109 and KYSE450 cells. (h and i) Representative migration (h) and invasion (i) analyses by transwell assay with transfected ECA109 and KYSE450 cells. (j) Migration evaluation by wound-healing assay with transfected ECA109 and KYSE450 cells. $^*p < 0.05$

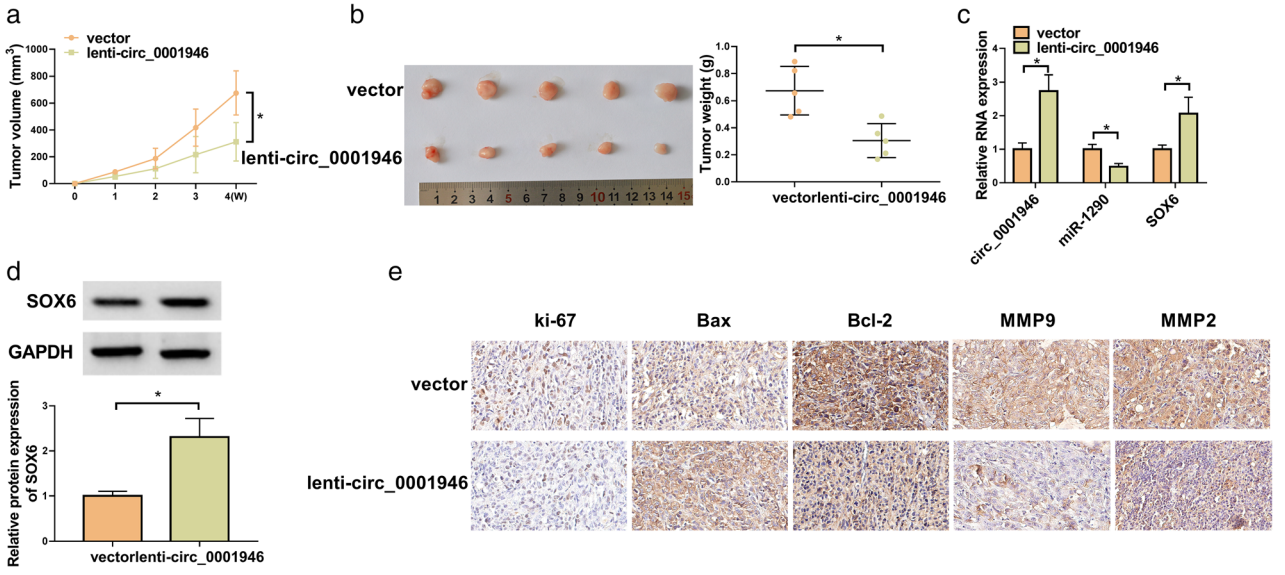

FIGURE 7 Circ_0001946 affects tumor growth in vivo. (a–e) ECA109 cells were infected by circ_0001946-expressing lentivirus (lenti-circ_0001946) or control lentivirus (vector). 5×10^6 infected cells were hypodermically implanted into the left flanks of the BALB/c nude mice ($n = 5$ per group). (a) Growth curves of the xenografts. Tumor growth was monitored for 4 weeks. (b) Images and average weight of the xenografts. (c) qRT-PCR showing the expression of circ_0001946, miR-1290 and SOX6 mRNA in the xenografts. (d) Representative immunoblotting analysis presenting SOX6 protein level in the xenografts. (e) Representative immunohistochemistry images showing ki-67, Bax, Bcl-2, MMP2, and MMP9 staining of sections of the xenografts. $^*p < 0.05$

Circ_0001946 expression suppresses the growth of ECA109 ESCC cells in vivo

In order to elucidate whether circ_0001946 can affect the growth of the xenograft in vivo, we infected human ECA109 ESCC cells with the circ_0001946-expressing lentivirus (lenti-circ_0001946) and hypodermically implanted into mice. Xenograft tumors derived from lenti-circ_0001946-transduced ECA109 cells showed smaller volume and average weight compared with the control ECA109 tumors (Figure 7a,b).

Moreover, qRT-PCR and immunoblotting analyses of the xenografts revealed that lenti-circ_0001946-transduced ECA109 tumors exhibited increased levels of circ_0001946 and SOX6 and reduced expression of miR-1290 compared with the control tumors (Figure 7c,d). Our immunohistochemistry analysis also supported the inhibition of the xenograft growth by circ_0001946 expression, as presented by the reduction of the cells stained with proliferating marker ki-67 in lenti-circ_0001946-transduced ECA109 tumors (Figure 7e). Additionally, lenti-circ_0001946-transduced ECA109 tumors had significantly greater cells stained with proapoptosis protein Bax, metastasis-related MMP9 and MMP2 proteins and fewer cells stained for antiapoptosis Bcl-2 than controls (Figure 7E), suggesting that circ_0001946 expression can promote cell apoptosis and impede metastasis. Taken together, these data reinforce our ectopic expression studies by identifying that circ_0001946 suppresses tumor growth in vivo.

DISCUSSION

Recently, abnormal up- and downregulation of circRNAs in human ESCC have been highlighted to affect ESCC pathogenesis.[14] Furthermore, the ceRNA activity of circRNAs in ESCC pathogenesis has begun to emerge.[5,10] For example, circ_0004771 is present at high levels in ESCC and it functions as a ceRNA for miR-339-5p to drive disease development by upregulating cell division cycle 25A (CDC25A).[40] CircZDHHC5 is capable of contributing to ESCC pathogenesis depending on the circZDHHC5/miR-217/zinc finger E-box binding homeobox 1 ceRNA crosstalk.[41] Conversely, circ-Foxo3 shows reduced expression in ESCC and can impede ESCC cell malignant behavior by involving the post-transcriptional modulation of PTEN via miR-23a competition.[42] Considering the anti-ESCC activity of circ_0001946,[14] we sought to explore its ceRNA mechanism in ESCC. Several recent studies have established a contradictory role of circ_0001946 in tumor biology,[11–13] which may be attributed to different tumor types or tumor microenvironments.

A classic example of circRNA-mediated ceRNA crosstalk involves the post-transcriptional RNA modulation via miRNAs.[8] In this report, we first unveiled that circ_0001946 can bind to miR-1290. Moreover, miR-1290 is a potent oncomir in ESCC.[23–26] Our findings first demonstrated that reduction of miR-1290 underlies circ_0001946-dependent phenotypes in ESCC cell lines. Similarly, circ_0001946 is reported to affect human tumorigenesis depending on its capacity to regulate specific miRNAs, such as miR-135a-5p and miR-671-5p.[11,12] Further studies to examine whether these miRNAs can participate in the regulation of circ_0001946 in ESCC are warranted.

SOX6 exerts a tumor-suppressive activity in human ESCC by affecting cancer cell apoptosis and proliferation.[30,31,39] Here, we ascertained for the first time that SOX6 is a miR-1290 target, and the ability of miR-1290 to affect ESCC cell phenotypes is attributable, at least in part, to its capacity to target SOX6. Consistent with our findings, miR-1269 and miR-208 function as strong oncomirs in ESCC by targeting and repressing SOX6.[31,32] Moreover, we first established that circ_0001946 involves SOX6 expression modulation via miR-1290 in a post-transcriptional manner. The function of SOX6 in gene modulation is multifaceted and intricate and can bind to DNA or interact with cofactors.[43–45] A future challenge will be to elucidate how the novel ceRNA crosstalk affects ESCC cell biological properties via SOX6. Additionally, although in vivo xenograft studies suggested that the inhibition of xenograft growth may be attributable to the upregulation of circ_0001946 and SOX6 and the reduction of miR-1290, the direct evidence of the circ_0001946/miR-1290/SOX6 ceRNA crosstalk in affecting tumor growth is lacking. Furthermore, the investigation about the influence of circ_0001946 on tumor metastasis in vivo is insufficient. Thus, further research is warranted.

To conclude, our findings uncover an undescribed molecular mechanism, the circ_0001946/miR-1290/SOX6 ceRNA crosstalk, in which circ_0001946 involves SOX6 expression regulation via miR-1290, for the anti-ESCC activity of circ_0001946. These findings suggest that a strategy directed toward restoring the expression of circRNAs with tumor suppressive functions might have a therapeutic value for ESCC.

CONFLICT OF INTEREST

The authors declare that they have no conflicts of interest.

ORCID

Li Wei https://orcid.org/0000-0003-4520-5221

REFERENCES

1. Bray F, Ferlay J, Soerjomataram I, Siegel RL, Torre LA, Jemal A. Global cancer statistics 2018: GLOBOCAN estimates of incidence and mortality worldwide for 36 cancers in 185 countries. CA Cancer J Clin. 2018;68:394–424.
2. Reichenbach ZW, Murray MG, Saxena R, Farkas D, Karassik EG, Klochkova A, et al. Clinical and translational advances in esophageal squamous cell carcinoma. Adv Cancer Res. 2019;144:95–135.
3. Jiang YY, Jiang Y, Li CQ, Zhang Y, Dakle P, Kaur H, et al. TP63, SOX2, and KLF5 establish a Core regulatory circuitry that controls epigenetic and transcription patterns in esophageal squamous cell carcinoma cell lines. Gastroenterology. 2020;159:1311–27.e19.
4. Sun Y, Qiu L, Chen J, Wang Y, Qian J, Huang L, et al. Construction of circRNA-associated ceRNA network reveals novel biomarkers for esophageal cancer. Comput Math Methods Med. 2020;2020:7958362.
5. Jiang C, Xu D, You Z, Xu K, Tian W. Dysregulated circRNAs and ceRNA network in esophageal squamous cell carcinoma. Front Biosci (Landmark Ed). 2019;24:277–90.
6. Kristensen LS, Andersen MS, Stagsted LVW, Hansen TB, Kjems J, Kjems J. The biogenesis, biology and characterization of circular RNAs. Nat Rev Genet. 2019;20:675–91.
7. Prats AC, David F, Diallo LH, Roussel E, Tatin F, Garmy-Susini B, et al. Circular RNA, the key for translation. Int J Mol Sci. 2020;21:8591.
8. Tay Y, Rinn J, Pandolfi PP. The multilayered complexity of ceRNA crosstalk and competition. Nature. 2014;505:344–52.

9. Kristensen LS, Hansen TB, Venø MT, Kjems J. Circular RNAs in cancer: opportunities and challenges in the field. Oncogene. 2018;37:555–65.
10. Shen Y, Shao Y, Niu C, et al. Systematic identification of circRNA-miRNA-mRNA regulatory network in esophageal squamous cell carcinoma. Front Genet. 2021;12:580390.
11. Deng Z, Li X, Wang H, Geng Y, Cai Y, Tang Y, et al. Dysregulation of CircRNA_0001946 contributes to the proliferation and metastasis of colorectal cancer cells by targeting MicroRNA-135a-5p. Front Genet. 2020;11:357.
12. Li X, Diao H. Circular RNA circ_0001946 acts as a competing endogenous RNA to inhibit glioblastoma progression by modulating miR-671-5p and CDR1. J Cell Physiol. 2019;234:13807–19.
13. Huang MS, Liu JY, Xia XB, Liu YZ, Li X, Yin JY, et al. Hsa_circ_0001946 inhibits lung cancer progression and mediates Cisplatin sensitivity in non-small cell lung cancer via the nucleotide excision repair signaling pathway. Front Oncol. 2019;9:508.
14. Fan L, Cao Q, Liu J, Zhang J, Li B. Circular RNA profiling and its potential for esophageal squamous cell cancer diagnosis and prognosis. Mol Cancer. 2019;18:16.
15. Islam F, Gopalan V, Lam AK. Roles of MicroRNAs in esophageal squamous cell carcinoma pathogenesis. Methods Mol Biol. 2020;2129:241–57.
16. Sang C, Chao C, Wang M, Zhang Y, Luo G, Zhang X. Identification and validation of hub microRNAs dysregulated in esophageal squamous cell carcinoma. Aging (Albany NY). 2020;12:9807–24.
17. Wei J, Yang L, Wu YN, Xu J. Serum miR-1290 and miR-1246 as potential diagnostic biomarkers of human pancreatic cancer. J Cancer. 2020;11:1325–33.
18. Liu X, Xu X, Pan B, He B, Chen X, Zeng K, et al. Circulating miR-1290 and miR-320d as novel diagnostic biomarkers of human colorectal cancer. J Cancer. 2019;10:43–50.
19. Wu Y, Wei J, Zhang W, Xie M, Wang X, Xu J. Serum Exosomal miR-1290 is a potential biomarker for lung adenocarcinoma. Onco Targets Ther. 2020;13:7809–18.
20. Qin WJ, Wang WP, Wang XB, Zhang XT, du JD. MiR-1290 targets CCNG2 to promote the metastasis of oral squamous cell carcinoma. Eur Rev Med Pharmacol Sci. 2019;23:10332–42.
21. Yan L, Cai K, Sun K, Gui J, Liang J. MiR-1290 promotes proliferation, migration, and invasion of glioma cells by targeting LHX6. J Cell Physiol. 2018;233:6621–9.
22. Ta N, Huang X, Zheng K, Zhang Y, Gao Y, Deng L, et al. miRNA-1290 promotes aggressiveness in pancreatic ductal adenocarcinoma by targeting IKK1. Cell Physiol Biochem. 2018;51:711–28.
23. Xie R, Wu SN, Gao CC, Yang XZ, Wang HG, Zhang JL, et al. Prognostic value of combined and individual expression of microRNA-1290 and its target gene nuclear factor I/X in human esophageal squamous cell carcinoma. Cancer Biomark. 2017;20:325–31.
24. Mao Y, Liu J, Zhang D, Li B. MiR-1290 promotes cancer progression by targeting nuclear factor I/X(NFIX) in esophageal squamous cell carcinoma (ESCC). Biomed Pharmacother. 2015;76:82–93.
25. Sun H, Wang L, Zhao Q, Dai J. Diagnostic and prognostic value of serum miRNA-1290 in human esophageal squamous cell carcinoma. Cancer Biomark. 2019;25:381–7.
26. Li M, He XY, Zhang ZM, Li S, Ren LH, Cao RS, et al. MicroRNA-1290 promotes esophageal squamous cell carcinoma cell proliferation and metastasis. World J Gastroenterol. 2015;21:3245–55.
27. Barbarani G, Fugazza C, Barabino SML, Ronchi AE. SOX6 blocks the proliferation of BCR-ABL1(+) and JAK2V617F(+) leukemic cells. Sci Rep. 2019;9:3388.
28. Marchetto A, Grünewald TGP. SOX6: a double-edged sword for Ewing sarcoma. Mol Cell Oncol. 2020;7:1783081.
29. Kambara T, Amatya VJ, Kushitani K, Suzuki R, Fujii Y, Kai Y, et al. SOX6 is a novel Immunohistochemical marker for differential diagnosis of Epithelioid mesothelioma from lung adenocarcinoma. Am J Surg Pathol. 2020;44:1259–65.
30. Qin YR, Tang H, Xie F, Liu H, Zhu Y, Ai J, et al. Characterization of tumor-suppressive function of SOX6 in human esophageal squamous cell carcinoma. Clin Cancer Res. 2011;17:46–55.
31. Li H, Zheng D, Zhang B, Liu L, Ou J, Chen W, et al. Mir-208 promotes cell proliferation by repressing SOX6 expression in human esophageal squamous cell carcinoma. J Transl Med. 2014;12:196.
32. Bai X, Wang Q, Rui X, Li X, Wang X. Upregulation of miR-1269 contributes to the progression of esophageal squamous cell cancer cells and is associated with poor prognosis. Technol Cancer Res Treat. 2021;20:1533033820985858.
33. Zhao Y, Zhang Q, Liu H, Wang N, Zhang X, Yang S. lncRNA PART1, manipulated by transcriptional factor FOXP2, suppresses proliferation and invasion in ESCC by regulating the miR-18a-5p/SOX6 signaling axis. Oncol Rep. 2021;45:1118–32.
34. Wang T, Kang W, du L, Ge S. Rho-kinase inhibitor Y-27632 facilitates the proliferation, migration and pluripotency of human periodontal ligament stem cells. J Cell Mol Med. 2017;21:3100–12.
35. Dudekula DB, Panda AC, Grammatikakis I, De S, Abdelmohsen K, Gorospe M. CircInteractome: a web tool for exploring circular RNAs and their interacting proteins and microRNAs. RNA Biol. 2016;13:34–42.
36. Lewis BP, Burge CB, Bartel DP. Conserved seed pairing, often flanked by adenosines, indicates that thousands of human genes are microRNA targets. Cell. 2005;120:15–20.
37. Tazawa H, Tsuchiya N, Izumiya M, Nakagama H. Tumor-suppressive miR-34a induces senescence-like growth arrest through modulation of the E2F pathway in human colon cancer cells. Proc Natl Acad Sci U S A. 2007;104:15472–7.
38. Iwakawa HO, Tomari Y. The functions of MicroRNAs: mRNA decay and translational repression. Trends Cell Biol. 2015;25:651–65.
39. Zhu Y, Xia Y, Niu H, Chen Y. MiR-16 induced the suppression of cell apoptosis while promote proliferation in esophageal squamous cell carcinoma. Cell Physiol Biochem. 2014;33:1340–8.
40. Huang E, Fu J, Yu Q, Xie P, Yang Z, Ji H, et al. CircRNA hsa_circ_0004771 promotes esophageal squamous cell cancer progression via miR-339-5p/CDC25A axis. Epigenomics. 2020;12:587–603.
41. Wang Q, Yang L, Fan Y, Tang W, Sun H, Xu Z, et al. Circ-ZDHHC5 accelerates esophageal squamous cell carcinoma progression in vitro via miR-217/ZEB1 Axis. Front Cell Dev Biol. 2020;8:570305.
42. Xing Y, Zha WJ, Li XM, Li H, Gao F, Ye T, et al. Circular RNA circFoxo3 inhibits esophageal squamous cell cancer progression via the miR-23a/PTEN axis. J Cell Biochem. 2020;121:2595–605.
43. Leow SC, Poschmann J, Too PG, Yin J, Joseph R, McFarlane C, et al. The transcription factor SOX6 contributes to the developmental origins of obesity by promoting adipogenesis. Development. 2016;143:950–61.
44. Iguchi H, Ikeda Y, Okamura M, Tanaka T, Urashima Y, Ohguchi H, et al. SOX6 attenuates glucose-stimulated insulin secretion by repressing PDX1 transcriptional activity and is down-regulated in hyperinsulinemic obese mice. J Biol Chem. 2005;280:37669–80.
45. Chen L, Xie Y, Ma X, Zhang Y, Li X, Zhang F, et al. SOX6 represses tumor growth of clear cell renal cell carcinoma by HMG domain-dependent regulation of Wnt/β-catenin signaling. Mol Carcinog. 2020;59:1159–73.

SUPPORTING INFORMATION

Additional supporting information may be found in the online version of the article at the publisher's website.

How to cite this article: Wang J, Yao W, Li J, Zhang Q, Wei L. Identification of a novel circ_0001946/miR-1290/SOX6 ceRNA network in esophageal squamous cell cancer. Thorac Cancer. 2022;13:1299–310. https://doi.org/10.1111/1759-7714.14381